Kinetic Study of the Insertion and Deinsertion of Carbon Dioxide into *fac*-$(CO)_3$(dppe)MnOR Derivatives

Donald J. Darensbourg,* Way-Zen Lee,† Andrea L. Phelps, and Erin Guidry

Department of Chemistry, Texas A&M University, College Station, Texas 77843

Received August 4, 2003

*Summary: The insertion of carbon dioxide into the Mn−O bond of fac-$(CO)_3$(dppe)MnOCH$_3$ (**1**) was observed to occur instantaneously at −78 °C by in situ infrared spectroscopy. The product of carboxylation of **1**, fac-$(CO)_3$(dppe)MnOC(O)OCH$_3$ (**2**), underwent decarboxylation with a first-order rate constant of 1.49×10^{-4} s^{-1} at 23 °C. The kinetic parameters for this process were determined by trapping the intermediate produced upon CO_2 extrusion, complex **1**, with COS to provide the very stable fac-$(CO)_3$(dppe)MnSC(O)OCH$_3$ (**3**) derivative. The structure of **3** was determined by single-crystal X-ray diffraction analysis, establishing the presence of the Mn−S bond.*

Introduction

A major focus of our current research is the catalytic coupling of carbon dioxide and epoxides to produce polycarbonates.[1] We and others have employed a variety of metal complexes as effective homogeneous catalysts or catalyst precursors for this environmentally benign synthesis of these biodegradable thermoplastics.[2] Fundamental to understanding the intimate mechanistic details of this process is a knowledge of the factors influencing the insertion of carbon dioxide into metal−oxygen bonds and its reverse deinsertion process (boxed portion of eq 1). We have in the past established for

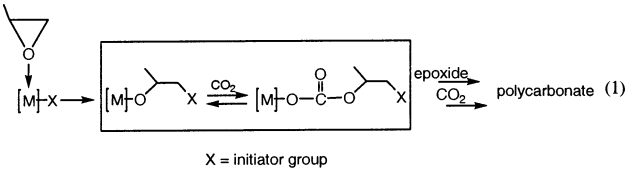

(1)

anionic group 6 metal carbonyl derivatives that this insertion reaction does not require a coordination site at the metal center. The reaction is proposed to involve the interaction of the weakly electrophilic carbon center of CO_2 with the lone pair on the oxygen atom of the alkoxide or aryloxide (OR groups).[3] That is, a four-centered transition state as depicted in **A** is suggested

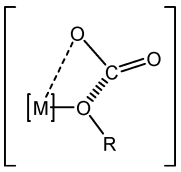

transition state

A

to occur along the insertion pathway. A similar conclusion was reached for an analogous insertion reaction involving CO_2 and CS_2 with neutral rhenium alkoxide complexes by Simpson and Bergman.[4] Consistent with this interpretation, it was further demonstrated that the insertion reaction was retarded in instances where there was steric hindrance around the oxygen atom, whether it be due to the steric bulk of R or an ancillary adjacent ligand.[5] However, there are few quantitative kinetic measurements for the insertion or deinsertion of CO_2 into M−OR bonds. In particular, it is of significance to quantify the rate of the insertion reaction as a function of the electronic nature of the R substituent on −OR.

In this communication we have chosen to investigate well-characterized and well-behaved complexes of Mn(I), as illustrated in eq 2, where dppe = bis(diphenylphosphino)ethane.[6] Although this system is not of

$$fac\text{-}(CO)_3(dppe)Mn(OCH_3) + CO_2 \underset{k_2}{\overset{k_1}{\rightleftharpoons}} fac\text{-}(CO)_3(dppe)Mn{-}OC(O)OCH_3 \quad (2)$$

* To whom correspondence should be addressed. Fax: (979) 845-0158. E-mail: djdarens@mail.chem.tamu.edu.

† Current address: Department of Chemistry, National Taiwan Normal University, No. 88, Sec. 4, Ting-Chow Rd., Taipei, Taiwan 116, ROC.

(1) For our most recent contribution to this subject, see: Darensbourg, D. J.; Rodgers, J. L.; Fang, C. C. *Inorg. Chem.* **2003**, *42*, 4498−4500.

(2) (a) Darensbourg, D. J.; Holtcamp, M. W. *Macromolecules* **1995**, *28*, 7577−7579. (b) Super, M.; Berluche, E.; Costello, C.; Beckman, E. *Macromolecules* **1997**, *30*, 368−372. (c) Super, M.; Beckman, E. *J. Macromol. Symp.* **1998**, *127*, 89−108. (d) Cheng, M.; Lobkovsky, E. B.; Coates, G. W. *J. Am. Chem. Soc.* **1998**, *120*, 11018−11019. (e) Beckman, E. *Science* **1999**, *283*, 946−947. (f) Darensbourg, D. J.; Holtcamp, M. W.; Struck, G. E.; Zimmer, M. S.; Niezgoda, S. A.; Rainey, P.; Robertson, J. B.; Draper, J. D.; Reibenspies, J. H. *J. Am. Chem. Soc.* **1999**, *121*, 107−116. (g) Darensbourg, D. J.; Wildeson, J. R.; Yarbrough, J. C.; Reibenspies, J. H. *J. Am. Chem. Soc.* **2000**, *122*, 12487−12496. (h) Cheng, M.; Moore, D. R.; Reczek, J. J.; Chamberlain, B. M.; Lobkovsky, B. E.; Coates, G. W. *J. Am. Chem. Soc.* **2001**, *123*, 8738−8749. (i) Cheng, M.; Darling, N. A.; Lobkovsky, E. B.; Coates, G. W. *Chem. Commun.* **2000**, 2007−2008. (j) Eberhardt, R.; Allmendinger, M.; Luinstra, G. A.; Rieger, B. *Organometallics* **2003**, *22*, 211−214. (k) Inoue, S. *J. Polym. Sci.: A* **2000**, *38*, 2861−2871. (l) Kruper, W. J.; Dellar, D. V. *J. Org. Chem.* **1995**, *60*, 725−727. (m) Mang, S.; Cooper, A. I.; Colclough, M. E.; Chauhan, N.; Holmes, A. *Macromolecules* **2000**, *33*, 303−308. (n) Allen, S. D.; Moore, D. R.; Lobkovsky, E. B.; Coates, G. W. *J. Am. Chem. Soc.* **2002**, *124*, 14284−14285. (o) Darensbourg, D. J.; Lewis, S. J.; Rodgers, J. L.; Yarbrough, J. C. *Inorg. Chem.* **2003**, *42*, 581−589. (p) Darensbourg, D. J.; Yarbrough, J. C. *J. Am. Chem. Soc.* **2002**, *124*, 6335. (q) Eberhardt, R.; Allmendinger, M.; Rieger, B. *Macromol. Rapid Commun.* **2003**, *24*, 194−196. (r) Darensbourg, D. J.; Yarbrough, J. C.; Ortiz, C.; Fang, C. C. *J. Am. Chem. Soc.* **2003**, *125*, 7586−7591.

(3) Darensbourg, D. J.; Sanchez, K. M.; Reibenspies, J. H.; Rheingold, A. L. *J. Am. Chem. Soc.* **1989**, *111*, 7094−7103.

(4) Simpson, R. D.; Bergman, R. G. *Angew. Chem., Int. Ed. Engl.* **1992**, *31*, 220.

(5) Darensbourg, D. J.; Mueller, B. L.; Bischoff, C. J.; Chojnacki, S. S.; Reibenspies, J. H. *Inorg. Chem.* **1991**, *30*, 2418−2424.

10.1021/om034087j CCC: $25.00
Publication on Web 11/15/2003

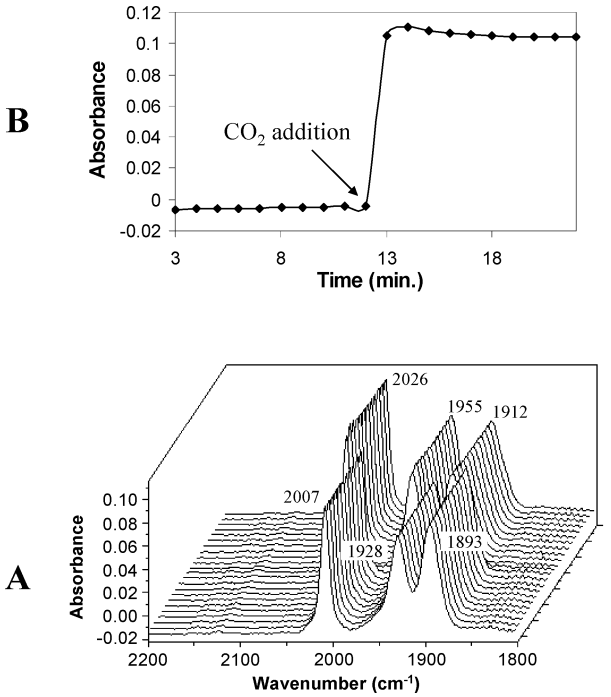

Figure 1. (A) Infrared traces in the ν(CO) region taken every 1 min for complex **1** in methylene chloride at −78 °C, before and after addition of CO_2. Infrared bands at 2007, 1928, and 1893 cm^{-1} are due to **1**, and bands at 2026, 1955, and 1912 cm^{-1} are due to **2**. (B) Absorbance of the ν(CO) band at 2026 cm^{-1} due to the product of CO_2 insertion, *fac*-$(CO)_3$(dppe)$MnOC(O)OCH_3$ (**2**), as a function of time before and after addition of CO_2.

catalytic importance, it allows for definitive assessment of the kinetic parameters and factors affecting this class of reactions. These observations should be highly transferable between various metal systems, including those relevant to catalytic CO_2/epoxide coupling reactions.

Results and Discussion

Mandal, Ho, and Orchin have previously reported that *fac*-$(CO)_3$(dppe)$MnOCH_3$ (**1**) is very reactive toward CO_2 to afford the corresponding methyl carbonate complex.[6b] Indeed, complex **1** was found to absorb CO_2 from the air both in solution and in the solid state. Consistent with these observations, we found that it was necessary to rigorously exclude adventitious sources of carbon dioxide during the preparation and isolation of complex **1** to avoid premature formation of *fac*-$(CO)_3$(dppe)-$MnOC(O)OCH_3$ (**2**). In an attempt to quantify the rate of carbon dioxide insertion into **1** in methylene chloride at −78 °C using an in situ infrared probe (see the Supporting Information), we were only able to establish a lower limit for the insertion rate. That is, when a CH_2-Cl_2 solution of **1** at −78 °C was exposed to an atmosphere of bone-dry CO_2, the instantaneous transformation **1** → **2** occurred. Figure 1 illustrates the infrared traces in the ν(CO) region of complex **1** prior to the addition of CO_2 and of complex **2** immediately after addition of CO_2. This experiment was performed by briefly bubbling CO_2 into a cooled solution of complex **1** via a syringe needle. Because of the rapidity of the insertion reaction, which was complete within 1 min, an accurate value for [CO_2] is not available. Nevertheless, it is certainly less than its concentration at saturation of ∼16 M at −78 °C.[7] Therefore, employing a [CO_2] value of 16 M and a $t_{1/2}$ value for the reaction of about 20 s allows us to calculate a lower limit for the second-order rate constant (k_1) of 2.0×10^{-3} M^{-1} s^{-1} at −78 °C. This value for the rate constant is probably grossly underestimated.

In a separate experiment a methylene chloride solution of complex **1** was stirred at ambient temperature in the presence of an atmosphere of ^{13}CO. Over an extended period of time *no* CO exchange of the ligands in complex **1** with free ^{13}CO in solution occurred. Furthermore, there was no indication of CO insertion into the Mn−OCH_3 bond under these conditions. *This observation is consistent with previous studies in this area, which have demonstrated that CO_2 insertion into metal−oxygen bonds occurs in the absence of a coordination site for prior CO_2 binding at the metal center.*

Reaction of the less electron-rich trifluoroethoxy derivative *fac*-$(CO)_3$(dppe)$MnOCH_2CF_3$ with a saturated methylene chloride solution of CO_2 was very slow at ambient temperature, whereas under these reaction conditions *no reaction* of *fac*-$(CO)_3$(dppe)MnO−2,6-dimethylphenoxide was observed. This is to be contrasted with the anionic tungsten carbonyl analogues, which were shown to readily react with CO_2 to afford the corresponding alkyl and aryl carbonate derivatives.[5] These observations add further credence to the premise that a very nucleophilic metal−oxygen center is required for reaction with the poorly electrophilic carbon dioxide molecule.

The kinetic parameters for the reverse process of eq 2, decarboxylation of the *fac*-$(CO)_3$(dppe)$MnOC(O)OCH_3$ complex (**2**), can be readily obtained by monitoring the reaction via two methods. The most obvious methodology would be to measure the rate of the CO_2 exchange process, as defined in eq 3, from either

$$fac\text{-}(CO)_3(dppe)MnO^{12}C(O)OCH_3 + {}^{13}CO_2 \rightleftharpoons fac\text{-}(CO)_3(dppe)MnO^{13}C(O)OCH_3 + {}^{12}CO_2 \quad (3)$$

direction. This procedure would require monitoring of the $\nu(CO_2)$ bands directly as shifted upon isotopic substitution. These vibrational modes are less intense than the ν(CO) stretches. Furthermore, there could be complications from the reverse process: i.e., eq 3 does not have a driving force. An alternative and more sensitive approach is to take advantage of the fact that COS extrusion from *fac*-$(CO)_3$(dppe)$MnSC(O)OCH_3$ (**3**) is not a facile process. Hence, we have determined the rate of CO_2 extrusion from complex **2** by trapping the decarboxylated complex **1** in the presence of a large excess of COS (Scheme 1).

Complex **3** has been independently synthesized and isolated in crystalline form for X-ray analysis. The complex crystallized, along with one molecule of methylene chloride, in the space group $P2_1/c$, as did the previously reported methoxy carbonate analogue.[6b] A thermal ellipsoid drawing of **3** is depicted in Figure 2. The molecular parameters in **3** are much like those

(6) (a) Mandal, S. K.; Ho, D. M.; Orchin, M. *Inorg. Chem.* **1991**, *30*, 2244−2248. (b) Mandal, S. K.; Ho, D. M.; Orchin, M. *Organometallics* **1993**, *12*, 1714−1719.

(7) Endre, B.; Bor, G.; Marta, M. S.; Gabor, M.; Bela, M.; Geza, S. *Veszpremi Vegyip. Egy. Kozl.* **1957**, *1*, 89−98.

Scheme 1

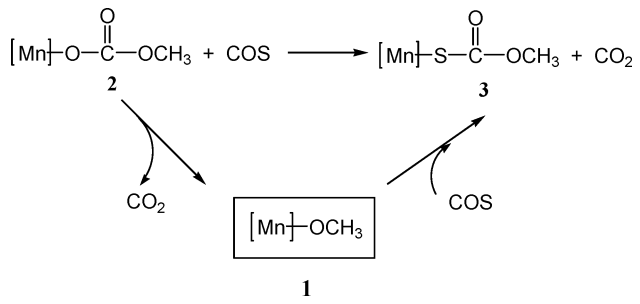

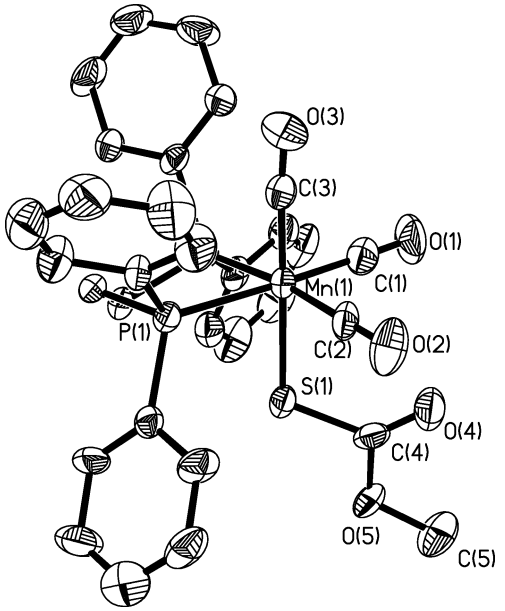

Figure 2. Thermal ellipsoid representation of complex **3**, *fac*-$(CO)_3$(dppe)Mn−SC(O)OCH_3.

reported for complex **2**. That is, the average Mn−P and Mn−CO_{eq} distances are 2.333(3) and 1.815(11) Å, respectively, in **3**, as compared with 2.34(1) and 1.82(1) Å in **2**.

Similarly, the Mn−CO_{ax} distance of 1.763(11) Å is shorter than the average Mn−CO_{eq} distance and is not significantly affected by being located trans to S as opposed to O in **2**, where the corresponding distance was determined to be 1.769(5) Å. The Mn−S bond length was found to be 2.363(3) Å, which is slightly shorter than the sum of the covalent radii (2.48 Å) of manganese and sulfur. A more complete listing of bond distances and bond angles in complex **3** may be found in the Supporting Information.

Figure 3 illustrates the three-dimensional stack plot of the infrared spectra taken in the ν(CO) and ν(COS) regions as a function of time, where the absorbance at 2043 cm^{-1} is due to COS. The carbonyl stretching vibrations in complex **2** at 2026, 1955, and 1912 cm^{-1} shift to 2020, 1955, and 1918 cm^{-1} upon replacing CO_2 with COS to afford **3**. The peak at 2026 cm^{-1} in complex **2** was used to calculate the first-order rate constants for **2** → **3** in the presence of a large excess of COS. Figure 3B depicts a typical trace for the disappearance of complex **2** as a function of time at 23 °C, along with a plot of its integrated form. The temperature-dependent first-order rate constants (k_2) and the derived enthalpy and entropy of activation values are listed in Table 1. As can be seen from these data, the release of CO_2 from

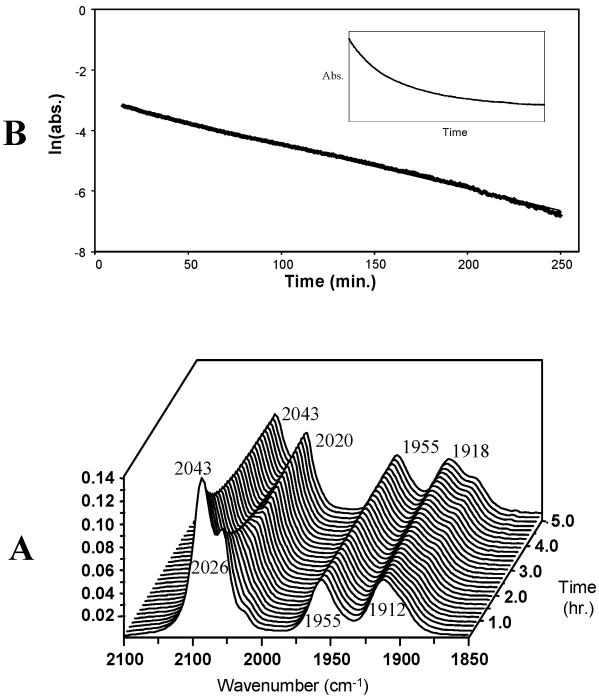

Figure 3. (A) Stack plot of infrared spectra as a function of time for the reaction described in Scheme 1. Infrared bands at 2026, 1955, and 1912 cm^{-1} are due to **2**, whereas bands at 2020, 1955, and 1918 cm^{-1} are due to **3**. The band for free COS is seen at 2043 cm^{-1}. (**B**) Absorbance vs time plot, as well as ln(absorbance) vs time plot for the disappearance of complex **2**.

Table 1. Temperature-Dependent Rate Constants and Activation Parameters for Decarboxylation of Complex 2[a]

temp (K)	$10^5 k_2$ (s^{-1})	$\Delta H^{\ddagger}$ (kJ/mol)	$\Delta S^{\ddagger}$ (J/(mol K))
273.1	0.185	130.0 ± 3.4	121.6 ± 11.9
282.9	1.16		
290.9	6.92		
296.2	14.9		
299.8	33.5		

[a] Reactions carried out in methylene chloride solution.

complex **2** is accompanied by a large positive entropy of activation (121.6 J/(mol K)), which is consistent with the loss of a stable small molecule. An extrapolation, with significant inaccuracy, of the data in Table 1 to −78 °C yields a k_2 value of 6.6×10^{-17} s^{-1}. Combining this k_2 with the estimated k_1 for the carboxylation reaction provides an equilibrium constant for **1** + CO_2 ⇆ **2** of $\geq 3 \times 10^{13}$ M^{-1} at −78 °C (or a ΔG value for reaction 2 of <-50 kJ/mol.). Hence, CO_2 insertion into the Mn−OCH_3 bond of complex **1** is kinetically and thermodynamically a highly favored process. Nevertheless, the kinetics of this reaction in general are extremely sensitive to the electronic nature of the substituents on the oxygen donor.

Summary

It is possible to glean some lessons from these and related studies relevant to the enchainment of CO_2 in the copolymerization of CO_2 and epoxides to provide polycarbonates. Important among these is more convincing evidence that CO_2 insertion into M−OR bonds does not require a site for CO_2 binding prior to insertion.

An even more pertinent observation is the dramatic differences in relative rates of CO_2 insertion into the Mn−OR moiety as a function of the R substituent, i.e., R = Me (very fast) > R = CH_2CF_3 (very slow) > R = O-2,6-$Me_2C_6H_3$ (not at all). Although these absolute rates will vary with the metal and its ancillary ligands, the relative order of reactivity is not expected to be altered. For example, Simpson and Bergman found *fac*-$(CO)_3(PMe_3)_2ReOCH_3$ to undergo carboxylation with CO_2 at −40 °C in less than 5 min, whereas the cresolate analogue was unreactive toward CO_2.[4] By way of contrast, the anionic aryloxide and fluoroalkoxide derivatives of tungsten carbonyl readily insert CO_2 at ambient temperature.[5,8] These results strongly suggest that epoxides bearing electron-withdrawing substituents in close proximity to the oxygen will be poor substrates for completely alternating copolymerization processes with carbon dioxide. Indeed, Rokicki and Kuran have reported the order of increasing oxirane reactivity in the copolymerization reaction with CO_2 employing zinc-based catalysts as follows: $ClCH_2$ < $C_6H_5CH_2$ < C_6H_5 < *n*-$C_4H_9OCH_2$ < H < CH_3.[9]

Experimental Section

All syntheses were carried out under argon using standard Schlenk and glovebox techniques. Solvents were distilled from the appropriate reagents before use. *fac*-$(CO)_3$(dppe)$MnOCH_3$ and *fac*-$(CO)_3$(dppe)$MnOC(O)OCH_3$ were prepared according to the literature.[6] Routine infrared spectra were measured on a Mattson Galaxy 6021 FT-IR spectrometer using a 0.1 mm CaF_2 sealed cell. NMR spectra were recorded on a Varian Unity Plus 300 MHz spectrometer. Kinetic measurements were monitored on ASI's ReactIR 1000 system equipped with an MCT detector and 30 bounce SiCOMP in situ probe.

The kinetic experiments were performed over the temperature range of 10−23 °C using 0.15 mmol of *fac*-$(CO)_3$(dppe)-$MnOC(O)OCH_3$ in 15 mL of dichloromethane and a large excess of COS. One spectrum was collected every 1 min for 5 h.

Preparation of *fac*-$(CO)_3$(dppe)$MnSC(O)OCH_3$ (3). A sample of *fac*-$(CO)_3$(dppe)$MnOCH_3$ dissolved in methylene chloride was stirred at ambient temperature over an atmosphere of COS for approximately 30 min. The solvent was removed under vacuum, and the yellow product was isolated. Crystals suitable for X-ray diffraction were grown by slow evaporation of a concentrated methylene chloride solution of **3** at ambient temperature. Anal. Calcd for $C_{31}H_{27}MnO_5P_2S\cdot CH_2Cl_2$ (713.43): C, 53.87; H, 4.10. Found: C, 54.01; H, 4.03.

X-ray Crystallography. A crystal of complex **3** was coated with a cryogenic protectant (i.e. Paratone) and mounted on a glass fiber, which in turn was fashioned to a copper mounting pin. The crystal was then placed in a cold nitrogen stream maintained at 110 K. The X-ray data were obtained on a Bruker CCD diffractometer and covered more than a hemisphere of reciprocal space by a combination of three sets of exposures; each exposure set had a different angle φ for the crystal orientation, and each exposure covered 0.3° in ω. The crystal-to-detector distance was 5.0 cm. Crystal decay was monitored by repeating the data collection for initial frames at the end of the data set and analyzing the duplicate reflections; crystal decay was negligible. The space group was determined on the basis of systematic absences and intensity statistics.

Table 2. X-ray Crystallographic Data for *fac*-$(CO)_3$(dppe)$MnSC(O)OCH_3$ (3)

empirical formula	$C_{31}H_{27}MnO_5P_2S\cdot CH_2Cl_2$
fw	713.39
temp (K)	110(2)
wavelength (Å)	0.710 73
space group	$P2_1/c$
a (Å)	8.761(2)
b (Å)	14.905(3)
c (Å)	25.230(5)
β (deg)	94.05
V (Å)^3	3286.4(12)
Z	4
D_{calcd} (g cm^{-3})	1.442
abs coeff (mm^{-1})	0.764
R^a	8.89
$R_w{}^b$	15.40
goodness of fit on F^2	1.028

^{a} $R = \sum||F_o| - |F_c||/\sum|F_o|$. ^{b} $R_w = \{[\sum w(F_o^2 - F_c^2)^2]/[\sum w(F_o^2)^2]\}^{1/2}$.

Crystal data and details of data collection are provided in Table 2. The structure was solved by direct methods (SHELXS, SHELTXL-PLUS program package, Sheldrick (1997)). Full-matrix least-squares anisotropic refinement for all non-hydrogen atoms yielded $R(F)$ and $R_w(F^2)$ values as indicated in Table 2 at convergence. All H atoms were placed at idealized positions and refined with fixed isotropic displacement parameters equal to 1.2 (1.5 for methyl protons) times the equivalent isotropic displacement parameters of the atoms to which they were attached. Neutral atom scattering factors and anomalous scattering factors were taken from Volume C of the International Tables for X-ray Crystallography.

Acknowledgment. Financial support from the National Science Foundation (Grant Nos. CHE 99-10342 and CHE 02-34860, and Grant No. CHE 98-07975 for purchase of X-ray equipment) and the Robert A. Welch Foundation is greatly appreciated.

Supporting Information Available: Complete details of the X-ray diffraction study of complex **3**, along with a table of selected bond distances and angles and a figure of the in situ infrared probe setup for the carbon dioxide insertion reaction study; crystallographic data are also available as CIF files. This material is available free of charge via the Internet at http://pubs.acs.org.

OM034087J

(8) Darensbourg, D. J.; Mueller, B. L.; Reibenspies, J. H.; Bischoff, C. J. *Inorg. Chem.* **1990**, *29*, 1789−1791.
(9) Rokicki, A.; Kuran, W. *J. Macromol. Sci. Rev. Macromol. Chem.* **1981**, *C21*, 135−186.